The role of shear and stabilizer on PLA degradation

Manuel Oliveira [a], Elsa Santos [a, b], Andreia Araújo [a], Guilhermino J.M. Fechine [c], Ana V. Machado [a], Gabriela Botelho [b, *]

[a] Institute of Polymers and Composites/I3N, University of Minho, Campus de Azurém, 4800-058 Guimarães, Portugal

[b] Centre/Department of Chemistry University of Minho, Campus de Gualtar, 4710-057, Braga, Portugal

[c] Graphene and Nano-materials Research Center - Mackgraphe, Mackenzie Presbyterian University, São Paulo, Brazil

Keywords:

Thermal stability
Poly(lactic acid)
Shear
B900 stabilizer
Molecular weight

Abstract

The role of temperature, shear and oxygen on PLA degradation was investigated. Thermo-mechanical degradation induces a larger decrease in PLA molecular weight than thermo-oxidative degradation. This was associated with different degradation processes (mainly chain scission) that took place under the two conditions. Given the PLA robustness to endure reprocessing, it was possible to conclude that the primary and secondary antioxidant (B900) had a synergetic effect on PLA stability.

Introduction

In the last decade, green chemistry, sustainability and environmental issues have been the main driving forces for the development of new materials, products and processes. Thus, the development of biodegradable polymers from renewable resources has been motivated by problems associated to the persistence of plastic in the environment, dwindling petroleum resources, shortage of landfill space and emission of toxic gases during incineration [1]. Nowadays, society is more motivated to use biodegradable plastics, not only as a way to solve the disposal problem of plastics in landfills, but also as a valid alternative to replace conventional polymers [2,3].

Aliphatic/aromatic polyesters, such as polylactic acid (PLA), polyhydroxybutyrate (PHB), polycaprolactone (PCL) and poly(butylene adipate terephthalate) (PBAT) are among the most popular biodegradable polymers [4]. PLA, obtained from renewable resources, is the most widely used biodegradable polymer in the world and the quantities produced start to answer industrial demands at competitive prices [3,5]. Besides presenting interesting qualities, such as good processability and good mechanical properties, it is suitable for many applications and also has low environmental impact, as shown in Life Cycle Analysis [6].

One of the main disadvantages of PLA is its thermal instability, reported since 1985, as a complex process [7]. It is enhanced by the presence of moisture, lactic acid residues, and metal catalysts and oxygen; the ester groups responsible for the biodegradation are also vulnerable to thermal degradation [2]. As known, thermal degradation occurs by random chain scission reactions, depolymerization, oxidative degradation, intramolecular and intermolecular transesterifications, hydrolysis, pyrolytic elimination and radical reactions [8,9]. As a result, molecular weight reduction occurs with the formation of lactide monomer and oligomers [10]. From the production point of view, these changes in PLA are undesired, not only because the material's melt viscosity and elasticity decrease, but also the processing equipment can be damaged due to the volatile lactide formation [3].

Since the main production processes of PLA are based on melt processing, especially extrusion and injection moulding which require high temperature and shear, it is crucial to understand the structural, thermal and rheological changes that can occur during these processes [11].

Several studies have been performed on PLA thermal degradation [12,13]. For example, Carrasco et al. determine the chemical structure, crystallinity, thermal stability and mechanical properties of PLA after processed by injection moulding [9]. They found that the crystalline structure almost disappears, ^{1}H and ^{13}C NMR confirmed that the chemical composition of PLA did not change, but the amount of methyl groups increased, which suggested the presence of a different molecular environment. However, there is a lack on studies that investigate the combination of temperature, shear and oxygen effects. Therefore, the main objective of this work was to investigate the role of temperature, shear and oxygen on PLA degradation. Moreover, the effect of a stabilizer addition during processing was also studied. Thus, two different methods were used; in the first, PLA films prepared by compression moulding were exposed to temperature and oxygen and, in the second, PLA pellets were processed in an internal mixer and samples were collected after different mixing times. PLA degradation was assessed by viscosity, ^{1}H Nuclear magnetic resonance spectroscopy (^{1}H NMR), infrared spectroscopy (FTIR), gel permeation chromatography (GPC) and differential scanning calorimetry (DSC).

Experimental

Materials

Commercial PLA grade (3251D) was supplied by NatureWorks LLC (USA) and according to Csikos et al. [14] it contains less than 2% D isomer and its density is 1.25 g cm^{-3}. PLA pellets were dried in a vacuum oven at 60°C for 12 h before use to prevent hydrolysis since this polymer is very hygroscopic. Tetrahydrofuran (THF), chloroform and deuterated chloroform were purchased from Lab-Scan and Acros Organics and used as received.

Stabilized PLA samples were prepared by adding 0.2%(w/w) [2] of B900, and its properties are indicated in Table 1.

Thermo-oxidative degradation

PLA pellets were pressed into thin films at 200°C under 30 ton for 60 s . The thickness of each film ($ca. 40 \mu$ m) was measured with a Mitutoyo pachymeter. The thin films were then cut into small rectangular sections (100×25 mm). Thermo-oxidative exposure of the samples was carried out in an oven under air at 140°C for 120 h .

Thermo-mechanical degradation

PLA was processed in a batch mixer (HAAKE Rheomix 600 OS; volume 69 cm [3]) equipped with two rotors running in a counterrotating way. The rotor speed was 100 rpm and the set temperature was 180°C. After a predetermined mixing time (from 5 to 25 min), the total sample was removed. The stabilizer (B900, 0.2wt%) was pre-mixed with the PLA pellets and then added together to the batch mixer chamber. As for PLA, these samples were processed during different time (from 5 to 25 min) and removed. Sample identification is presented in Table 2.

Characterization

2.4.1. ^{1}H Nuclear magnetic resonance spectroscopy (^{1}H NMR) ^{1} H NMR spectra of initial and degraded PLA samples were recorded on a Bruker Avance III 400 MHz spectrometer using deuterated chloroform as solvent and tetramethylsilane as internal standard.

Fourier transform infrared spectroscopy (FTIR)

Room temperature infrared spectra of the initial and degraded films were recorded on a Jasco spectrometer using ATR mode in the range $4000-600 \mathrm{~cm}^{-1}$ by averaging 64 scans and using a resolution of $8 \mathrm{~cm}^{-1}$. The peaks height ratios were determined using the mathematical expressions proposed by Sabnis and Block (equation (1)) [15]:

$$\text{Peak height ratio} = \frac{H_{\text{Peak X}}}{H_{\text{Ref Peak } (1455 \mathrm{~cm}^{-1})}}$$

where H_{Peak} x and $H_{\text{Ref Peak}}$ are the height of study peak and reference peak, respectively, determined using equation (2):

$$H_{\text{Peak}} = \log_{10} \frac{AC}{BC} \tag{2}$$

where AC is the height for the base line and BC is the absolute height of the absorption band of the functional groups at the respective wavenumber.

Viscosimetry

The intrinsic viscosity (η) of all samples (initial and degraded) was determined using an Ubbelohde capillary viscometer, with 5mg/mL solutions in chloroform at $25.0 \pm 0.5^{\circ}\mathrm{C}$ and according to equation (3) [16]:

$$\eta = \frac{\sqrt{2\left((\eta_r - 1) - \ln\ \eta_r\right)}}{c} \tag{3}$$

where η_r is the relative viscosity and c is polymer solution concentration. Five measurements were performed and averaged to obtain the solution viscosity of each sample.

Differential scanning calorimetry (DSC)

Thermal properties were determined in a Perkin-Elmer DSC Diamond under nitrogen. Approximately 6 mg of each sample were cut from the films and placed in an aluminium pan. The analysis was performed in three steps: first, heating from 30 to 200°C at 50°C/min, cooling from 200 to 30°C at 10°C/min, and second, heating from 30 to 200°C at 10°C/min. Two minute isothermal plateau were inserted between the ramps. Each sample was measured twice, indicating an experimental error of 0.5°C. The melting temperature (T_m) and melting enthalpy (ΔH_m) were determined from the second heating curves. The crystallinity degree (χ_c) was obtained using equation (4):

$$\chi_C(\%) = \left(\frac{\Delta H_m - \Delta H_{CC}}{\Delta H_m^0 \times \left(1 - \frac{wt\%B900}{100}\right)}\right) \times 100 \tag{4}$$

where ΔH_m and ΔH_{cc} are, respectively, the experimental melting enthalpy and the cold crystallization enthalpy obtained for the samples, ΔH_m^0 is the melting enthalpy of the 100% PLA (93.0 J/g) [17] and wt% B900 is the weight percentage of the incorporated stabilizer.

Table 1

B900 properties.

IUPAC/commercial name	Antioxidant type	M_w(g/mol)	% (w/w)	Melting temperature (°C)
Tris(2,4-di tert.butylphenyl)phosphite/IRGAFOS 168	Secondary	646.9	80	183-186
Octadecyl-3-(3,5-di-tert.butyl-4-hydroxyphenyl)-propionate/IRGANOX 1076	Primary	531	20	50-55

Table 2
Samples identification.

Samples	Identification
PLA -120 h	PLA exposed to thermo-oxidation during 120 h

PLA $-5,10,15,20,25$ min	PLA processed during 5,10,15,20 and 25 min
PLA + B $900-5,10,15,20,25$ min	PLA + B900 processed during 5,10,15,20 and 25 min

Gel permeation chromatography (GPC)

The number ($\mathrm{M_n}$) and weight average ($\mathrm{M_w}$) molar mass and polydispersity index (PDI) were measured by GPC. Solutions were prepared in THF (99.9%) and prefiltered on filter plate (hydrophobic polytetrafluoroethylene, 0.45μ m pore size) before injection. A Waters Alliance GPC Model 2695, equipped with 3 PLgel MIXED-B columns (inner diameter = 7.5 mm, length $= 30$ mm and particle size $= 10\mu$ m) and a Waters 2410 Differential Refractometer as detector, were used for the determination. THF was used as eluent with a flow rate of 1 mL/min and the temperatures were 25 and $35\,^{\circ}\mathrm{C}$ at the injector and detector, respectively. The molecular weights and PDIs were derived from a calibration curve based on narrow polystyrene standards.

Results and discussion

PLA degradation: role of temperature, oxygen and shear

^{1} H NMR analyses were performed for initial PLA, PLA after 25 min of processing and after 120 h of thermo-oxidative. The chemical shifts (δ) values obtained in the $^{1}\mathrm{H}$ NMR spectra, corresponding groups and integration values are listed in Table 3. It can be noted that the assignments obtained are in good agreement with Liu and co-workers results [18].

No changes in chemical shift values were observed between samples before and after processing. However, there are some differences in the signal intensities and in proton area ratio ($\mathrm{CH_3}/\mathrm{CH}$) for the samples processed, which slightly increase due to degradation, indicating that chain scission has occurred during processing. This ratio has a theoretical value of 3 and it must remain constant if degradation takes place due to ester linkage scission, hydrolysis or radical degradation, among others. This can explain the value obtained for samples submitted to thermal treatment. According to Carrasco and co-workers [9], who processed PLA by injection moulding, only pyrolytic elimination (which is responsible for the transformation of $\mathrm{CH}-\mathrm{CH_3}$ into $\mathrm{CH}=\mathrm{CH_2}$) can be responsible for a different ratio. Since, in the present work, there was no $\mathrm{CH_2}$ protons signal in $^{1}\mathrm{H}$ NMR, this mechanism, if present, must be secondary or of minor importance during the thermal degradation. Thus, the structural changes caused by thermomechanical and thermo-oxidative treatments were established by comparing the FTIR peaks height ratios of PLA, Fig. 1. Three bands were related to PLA degradation: $\mathrm{C}=\mathrm{O}$ stretching (around $1750\ \mathrm{cm}^{-1}$) and C-O stretch (1185 and $1090\ \mathrm{cm}^{-1}$) [2,19]. To obtain comparable results without experimental influence, the height ratios of the three peaks were determined related to the height of the reference peak at $1455\ \mathrm{cm}^{-1}$ (see equation (1) in experimental section), which is assigned to the $\mathrm{CH_3}$ deformation and known to be

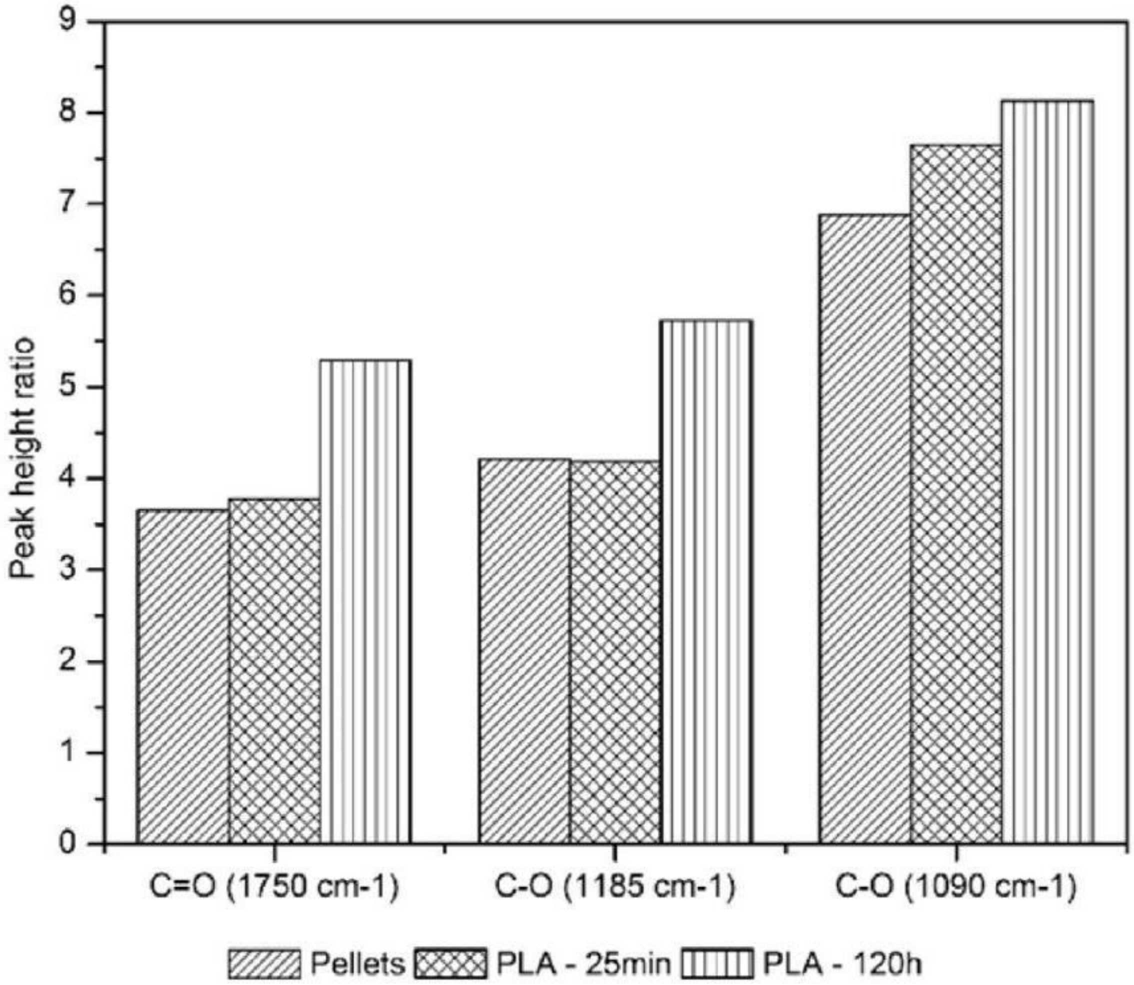

Fig. 1. FTIR peaks height ratio of PLA degradation characteristic bands.

suitable as internal standard for PLA. PLA was shown to be slightly sensitive to thermo-mechanical degradation. Among the three bands studied, only the C-O stretch at 1090 cm^{-1} suffered a small increase. Also, the crystalline carbonyl vibration of PLA, 1755 cm^{-1}, cannot clearly be identified in the spectrum (Fig. 2a), however the appearance of the hydroxyl band (3400 cm^{-1}) indicates occurrence of hydrolysis degradation.

After expose to thermo-oxidative conditions, the FTIR peaks height ratios increase for ester groups associated with the formation of new carbonyl compounds, both in the middle and at the end of chains [12]. This can be due to chain oxidation caused by the synergetic effect of temperature and oxygen, provoking cleavage of the long chains into shorter ones via the degradation mechanisms (hydrolysis, random chain-scission, trans-esterification, β-scission ...) together with a significant increase of carboxyl end groups [10]. Moreover, a new absorption band can be seen at 920 cm^{-1}, characteristic of vinyl unsaturated groups, and an increase to the unfolding band around 700 cm^{-1}, which corresponds to $C = O$ double bond (Fig. 2b) [20].

Since the increase of the PLA hydroxyl band after processing is not significant, it seems that degradation occurs mainly by chain scission. Therefore, the presence of moisture results in molecular weight reduction, following the mechanism proposed by Racha AlItry (Scheme 1) [10].

Table 3
^{1} H NMR data for PLA samples.

Samples	δCH_3 (ppm)	Integration	δCH (ppm)	Integration	Proton intensity ratio (CH_3/CH)
PLA pellet	1.56-1.60	78.76	5.14-5.21	21.24	3.04
PLA - 25 min	-	-	-	-	3.20
PLA - 120 h	1.58-1.60	74.81	5.13-5.21	25.19	2.97

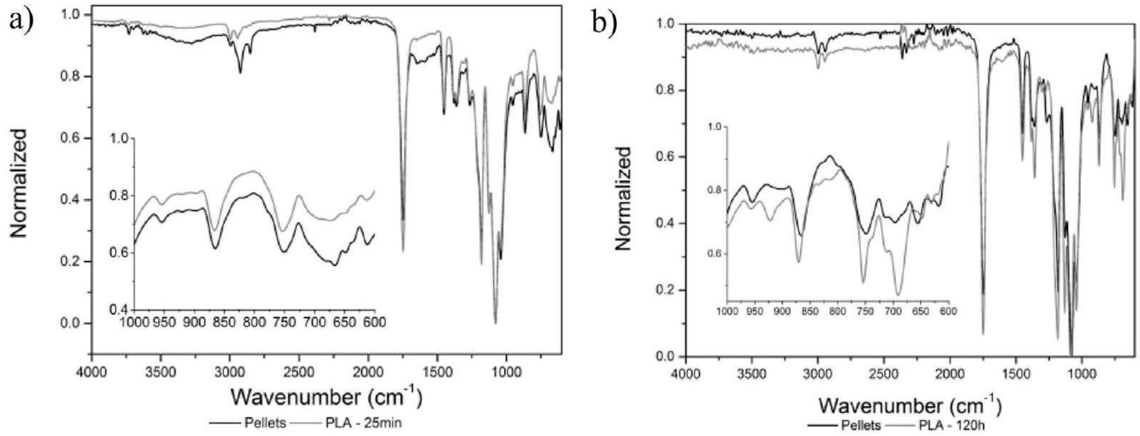

Fig. 2. FTIR spectra of PLA obtained before and after a) 25 min of processing and b) 120 h thermo-oxidative conditions.

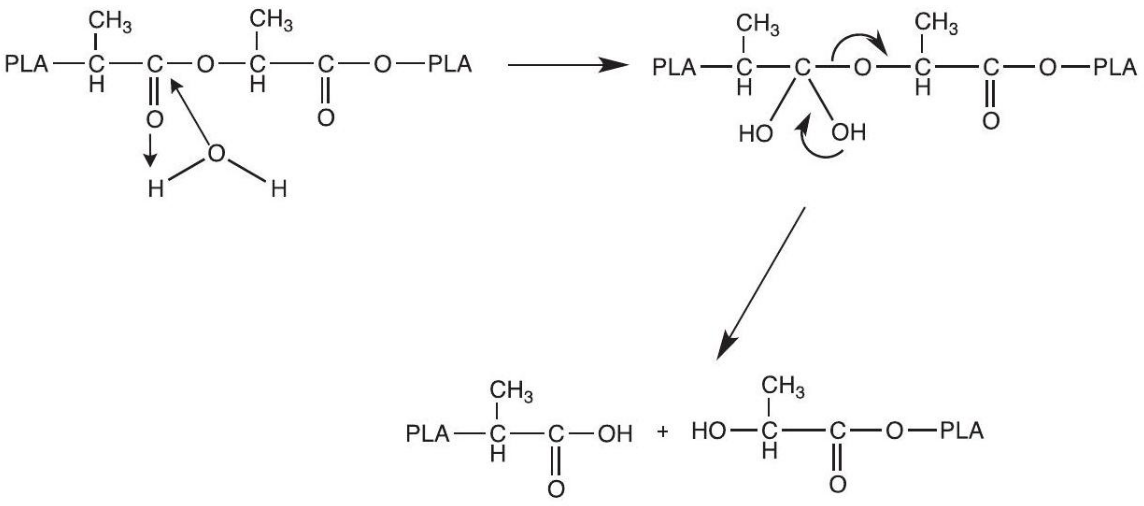

Scheme 1. Proposed degradation mechanisms of PLA by hydrolysis.

Consequently, to have a clear picture of the degradation extension, the intrinsic viscosity and crystallinity were assessed, and the results are shown in Fig. 3. A significant level of molecular degradation occurred, either when PLA was processed in the batch mixer or exposed to thermo-oxidative environment. It is known that shorter chains have higher mobility and can reorganize easily leading to an increase of crystallinity degree. Moreover, aging can also contribute to this. Chain scission occurrence is confirmed by the higher degree of crystallinity and lower intrinsic viscosity of the processed samples. This is in agreement with FTIR results, which showed more PLA chain scission during processing than during thermo-oxidative. This can be explained by the combined effect of high shear and temperature. While the decrease in viscosity caused by thermo-mechanical degradation was due to high temperature, oxygen and shear during melt mixing, during thermo-oxidative exposure, chain scission occurred by the synergetic effect of temperature and oxygen, resulting in oxidative degradation. Based on the results presented above, shear has a crucial role in PLA degradation mechanisms during processing.

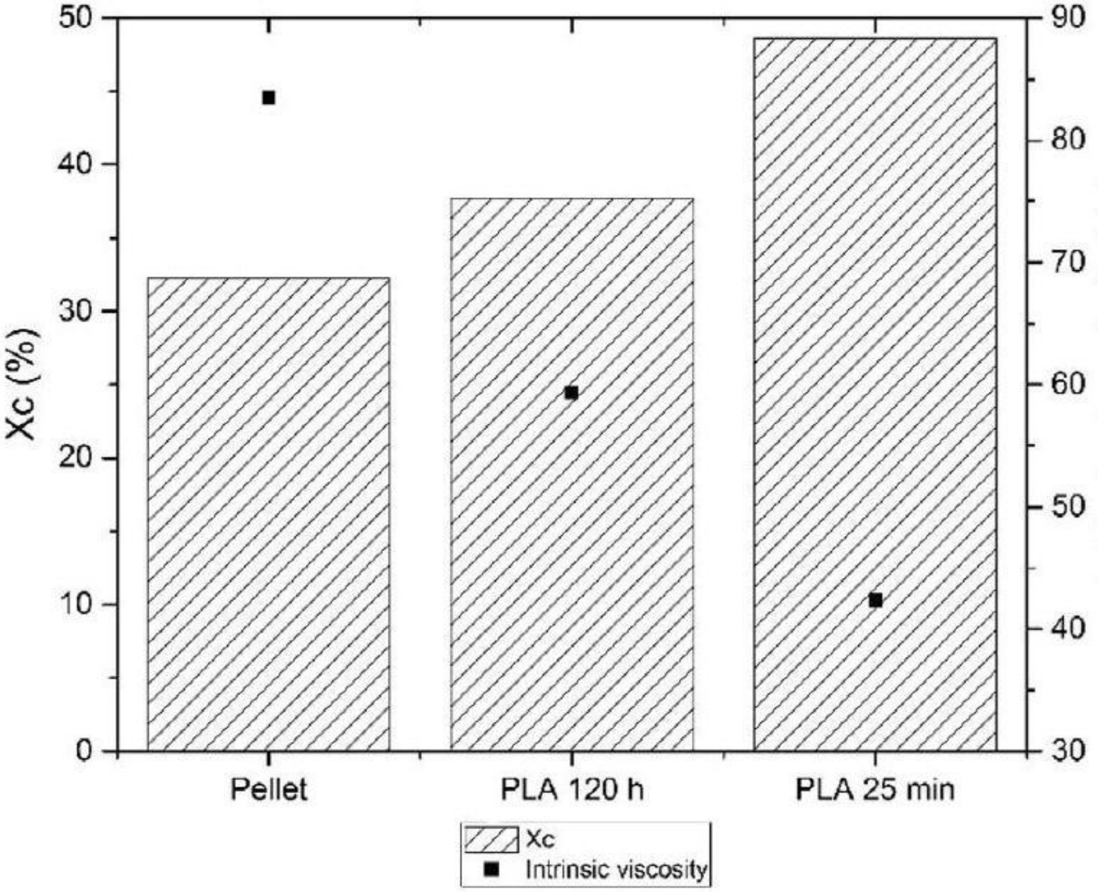

Fig. 3. PLA crystallinity and intrinsic viscosity after processing and exposure to thermal-oxidative conditions.

The reaction mechanism of PLA thermo-degradation was explained by McNeill and Leiper [21] who assumed that, under these conditions, the main reaction is non-radical with intramolecular trans-esterification, depending on the point in the polymer backbone where this reaction occurs. The final product could be a lactide molecule (Scheme 2a), an oligomeric ring with more than two repeat units (Scheme 2b) or acetaldehyde plus carbon monoxide (Scheme 2c). The McNeill and Leiper work supports that radical reaction just occurs at temperatures above 270°C, leading to a decrease in molecular weight. Although the temperature used in present work, either for processing or thermooxidative exposure, was lower than that, such reactions might occur due to the synergetic effect of shear and oxygen [2]. Scheme 3 represents the synergetic effect of temperature and oxygen. Temperature leads to PLA macroradicals formation that react with oxygen, developing peroxyl macroradicals (3a and 3c). These could react with macromolecules (PH) giving hydroperoxides (3b and 3d). The latter can easily suffer homolytic cleavage of the O – O bond, forming new free radicals that provoke chain scission or crosslinking.

2a

2b

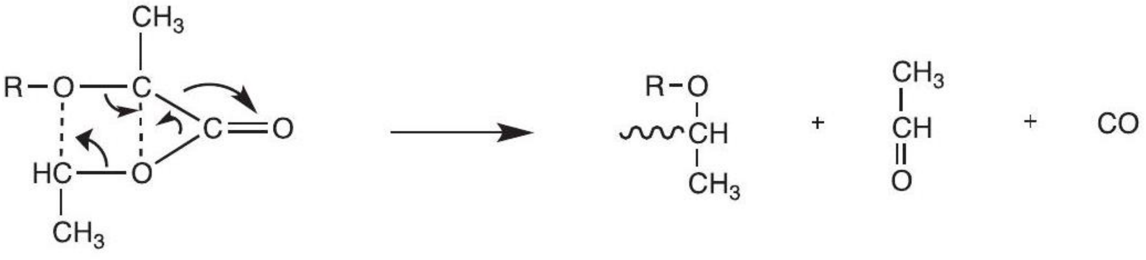

2c

Scheme 2. Nonradical reactions of PLA degradation presented by McNeill and Leiper [20].

PLA degradation: effect of stabilizer

To reduce or minimize the shear/temperature effect during processing, a stabilizer (B900) was added to PLA. This stabilizer acts directly on the deactivation of free radicals and on hydroperoxide decomposition. These are considered "primary" and "secondary" if they are hydrogen donors or hydroperoxide decomposers, respectively (Scheme 4). B900 is a mixture of Irganox 1076, a primary stabilizer and Irgafos 168, a secondary antioxidant. PLA is sensitive

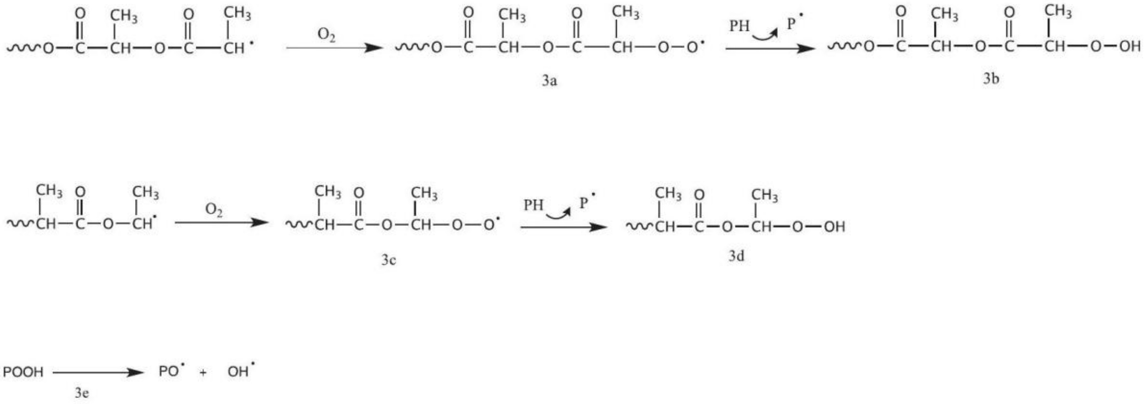

Scheme 3. Hydroperoxide formation and decomposition during the thermo-oxidation of PLA.

$$\mathrm{P^\circ + XH \rightarrow PH + X^\circ}$$

4a

$$(4b)\mathrm{POO^\circ + XH \rightarrow POOH + X^\circ}$$

$$\mathrm{POOH + YH \rightarrow Y = O + POH}$$

Scheme 4. Stabilization mechanism of primary (a and b) and secondary stabilizers (c) [2]. to radical and nonradical degradation and, as it was presented above, shear imposed during melting and mixing process enhances degradation. Adding this stabilizer, B900, is expected to minimize the molecular weight decrease during processing.

Fig. 4 depicts the evolution of carbonyl groups of PLA and PLA + B900 with processing time. As expected, and taking into account the experimental error, for PLA, the trend line associated with the peak height ratio of carbonyl group has a positive slope, indicating chain scission and oxidation occurred to some extent. On the contrary, the presence of stabilizer seems to prevent chain cleavage provoked by radical reactions (Scheme 3), as the trend lines are constant.

The stabilizer effect was evaluated based on molecular weight analysis, therefore the intrinsic viscosity was measured at different times during processing (Fig. 5). Since this method has higher sensibility to chain scission than FTIR, it was possible to observe that the intrinsic viscosity of neat PLA decreased linearly (around 50%) with processing time, due to the synergetic effect of shear, temperature and oxygen. The addition of stabilizer clearly changed this tendency. The intrinsic viscosity decreased around 27% up to 5 min , which could be attributed to non-radical reactions (Scheme 1), since the stabilizer cannot prevent its occurrence. Moreover, Fig. 5 also shows that, as the intrinsic viscosity decreases, the crystallinity increases. As expected, B900 stabilizes PLA, minimizing its degradation with processing time.

DSC heating curves obtained after erasing thermal history (i.e.

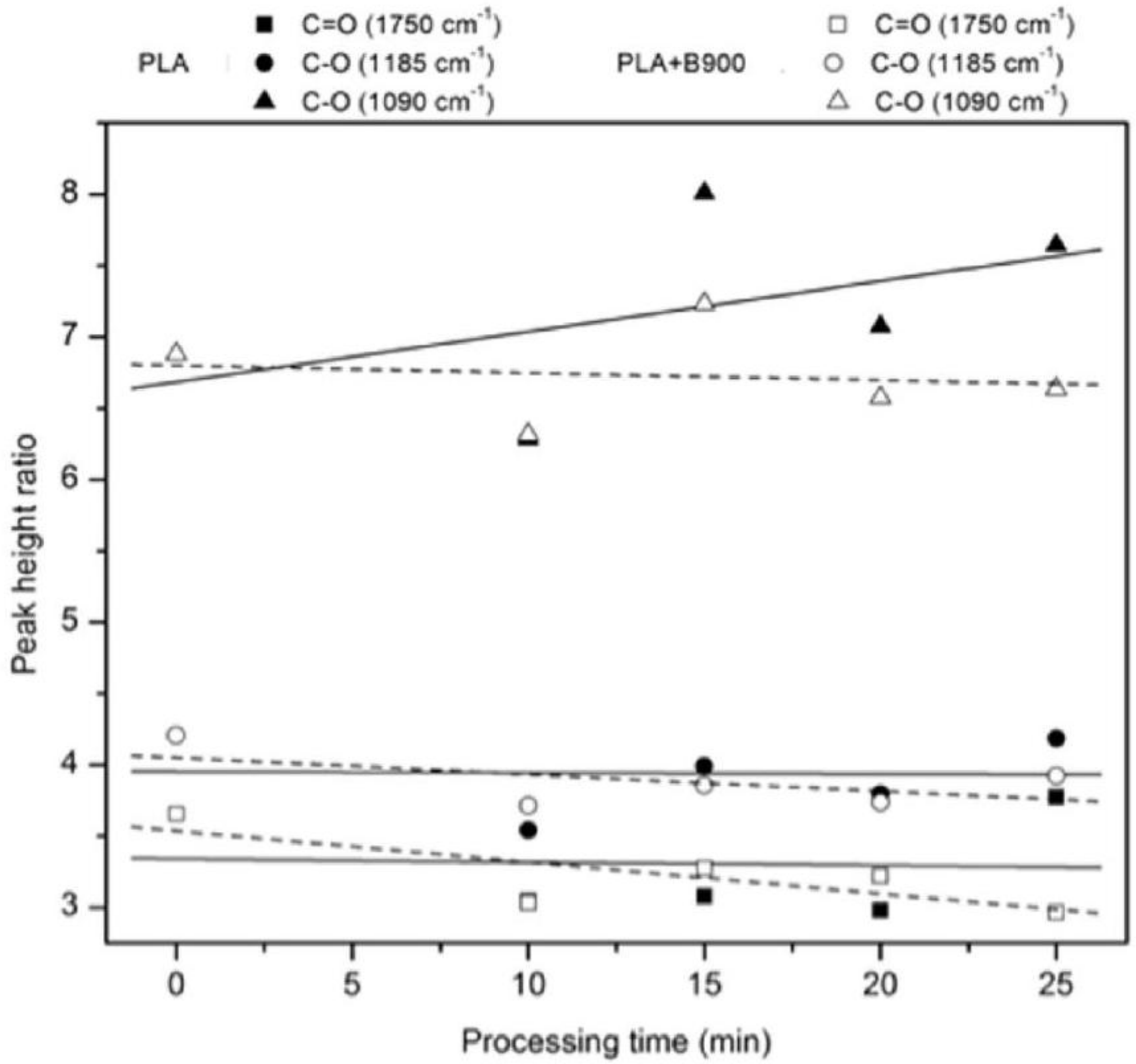

Fig. 4. Effect of stabilizer on carbonyl group formation during processing.

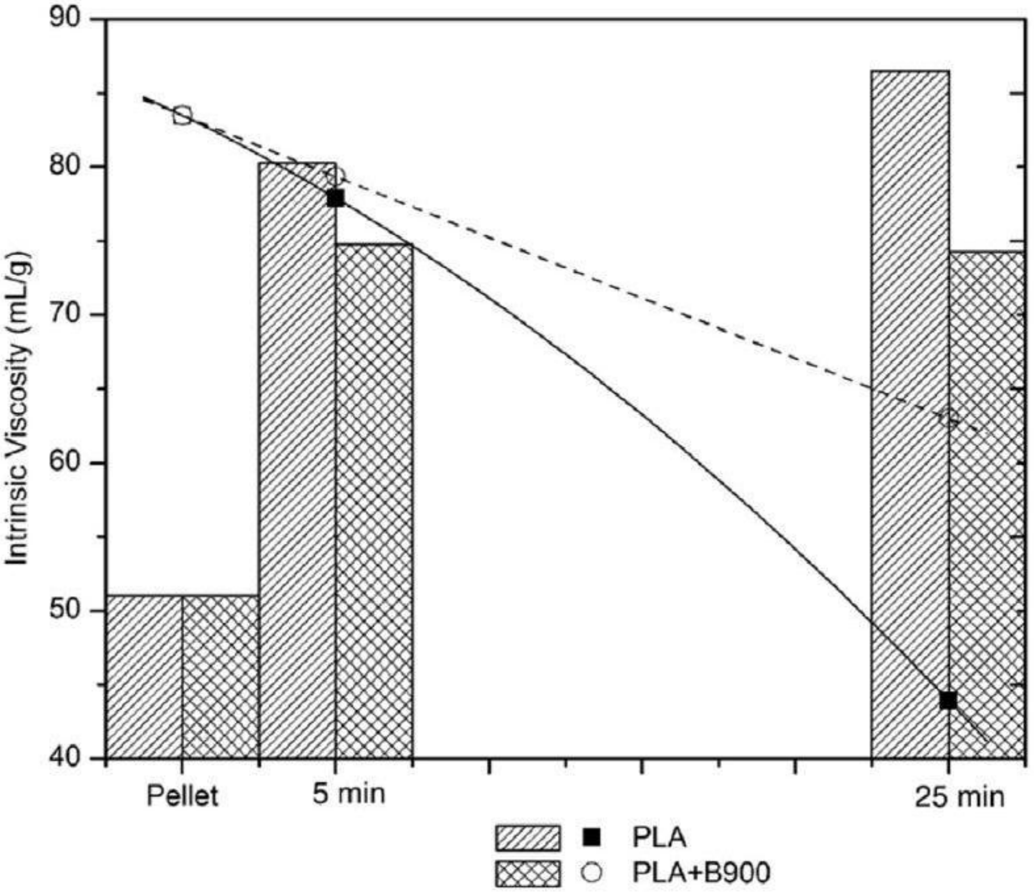

Fig. 5. Effect of stabilizer on PLA crystallinity (graph bars) and intrinsic viscosity (graph lines) along processing time.

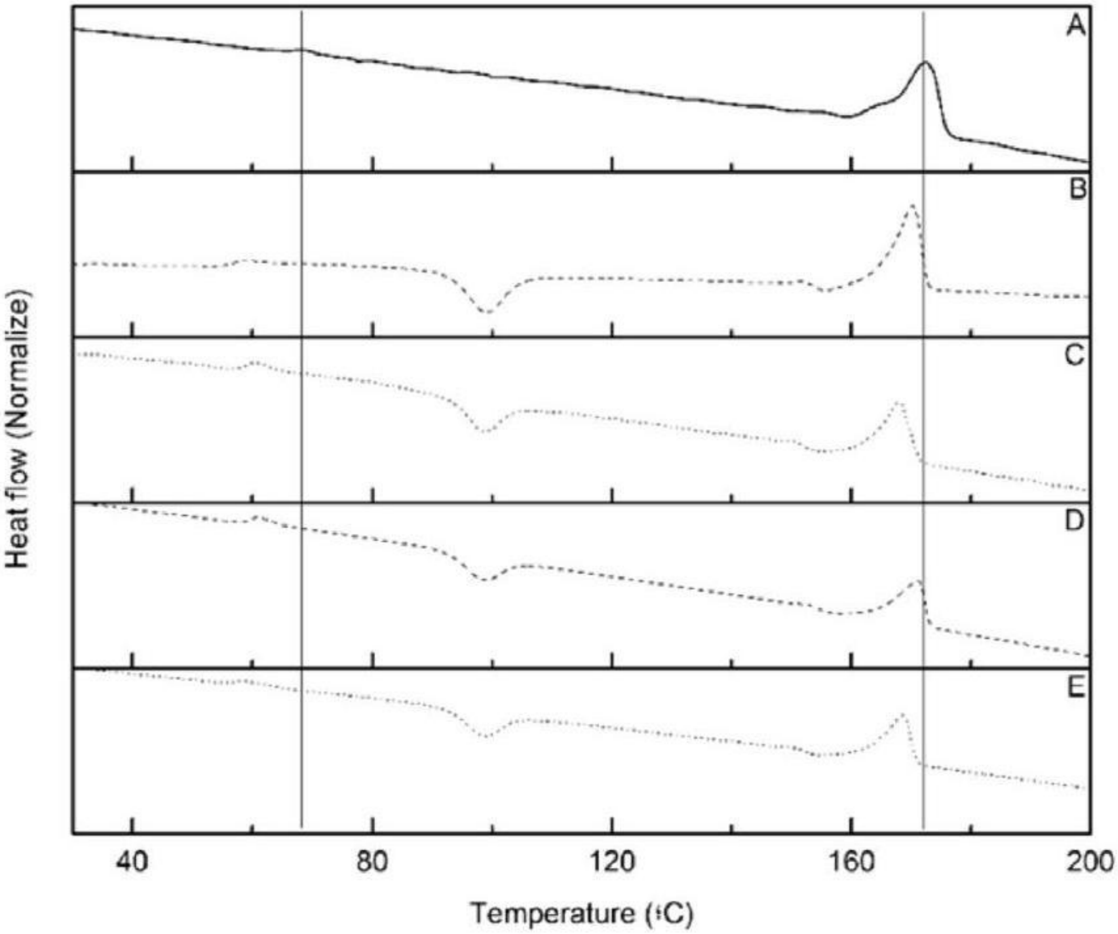

Fig. 6. DSC curves of neat PLA and PLA reprocessed at 180°C in the presence and absence of B900: A, PLA pellet; B, PLA - 5 min ; C, PLA - 25 min ; D, PLA + B900 - 5 min and E, PLA + B900 − 25 min.

2nd heating) are shown in Fig. 6, and the parameters calculated from those are depicted in Table 4. As can be seen, the processed PLA samples exhibit a decrease in the melting temperature (Tm), an increase in the melting enthalpy and, consequently, an increase in crystallinity. This can be due to chain scission leading to shorter molecular chains and reorganization of amorphous domains into crystalline ones, indicating an increase on molecular flexibility and

Table 4
DSC parameters for the thermal transitions observed to PLA and PLA + B900.

Samples	T_m PLA(°C)	ΔH_m(J/g)	χ_c(%)
PLA pellet	172.5	32.0	34.4
PLA -5 min	170.2	42.9	46.1
PLA -25 min	168.0	45.2	48.6
PLA + B900 -5 min	171.2	40.8	43.9

PLA + B900 -25 min	168.6	40.6	43.7

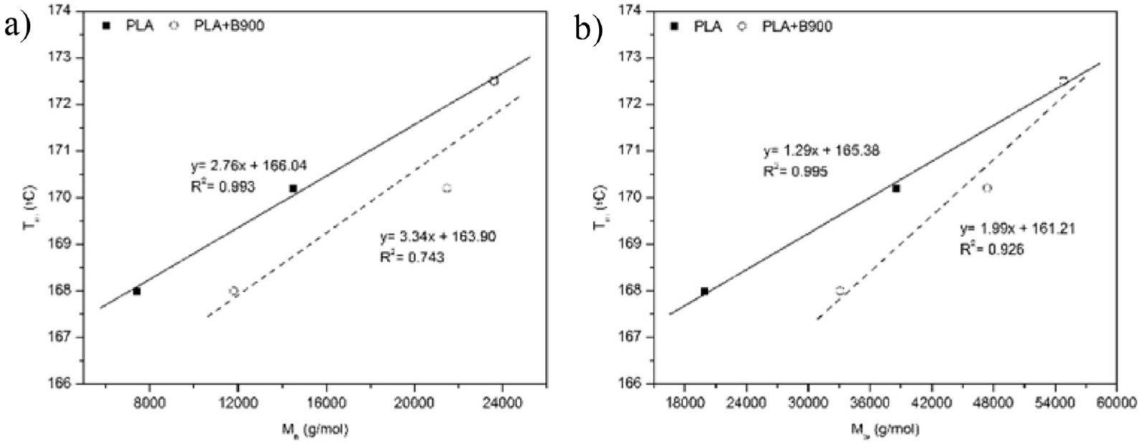

Fig. 7. Variation of PLA melting temperature (T_m) with average molecular weight for neat and processed materials; a) M_n, b) M_w.

mobility [9,22]. When B900 was added, the PLA crystallinity increase is less noticeable, corroborating the results discussed before.

To investigate the effect of B900 more deeply, size exclusion chromatography tests were performed and correlated with T_m. Fig. 7 indicates excellent relationship between the melting temperature and average molecular weight of PLA. An increase on processing time led to a decrease in average number molecular weight and, consequently, on T_m. While for PLA the average molecular weight decreases from 54834 to 19979 g/mol, for PLA with B900 the value reaches 33096 g/mol. The presence of B900 minimize, as expected, the molecular weight decrease of PLA when exposed to the melting temperature, shear and oxygen.

Similar behavior was observed for average number molecular weight, that decreased from 23612 to 7398 and 11799 g/mol for PLA and PLA with stabilizer, respectively.

Conclusions

The thermo-mechanical and thermo-oxidative degradation of PLA was evaluated. Coupling several characterization techniques, it was concluded that PLA is more sensitive to thermo-mechanical degradation, which is related to temperature-shear combination during processing. Moreover, it was shown that the presence of B900 minimizes the PLA degradation during consecutive processing cycles, preventing chain scission.

Acknowledgements

The authors acknowledge the n-STeP - Nanostructured systems for Tailored Performance, with reference NORTE-07-0124-FEDER000039, supported by the Programa Operacional Regional do Norte (ON.2), PEst-C/CTM/LA0025/2013 (Strategic Project - LA 25 -2013-2014) and PEST-C/QUI/UI0686/2013. Acknowledges are also due to the NMR Portuguese network (PTNMR, Brucker Avance III 400-Univ. Minho). GJMF is grateful to

FAPESP (Process 2010/076519) and CNPq (Process 304902/2012-8) Brazilian funding agencies for the financial support.

References

[1] M.A. Abdelwahab, A. Flynn, B.S. Chiou, S. Imam, W. Orts, E. Chiellini, Thermal, mechanical and morphological characterization of plasticized PLA-PHB blends, Polym. Degrad. Stab. 2012 (9) (1822) 97.
[2] N.S.Q.S. Amorin, G. Rosa, J.F. Alves, S.P.C. Gonçalves, S.M.M. Franchetti, G.J.M. Fechine, Study of thermodegradation and thermostabilization of poly(lactide acid) using subsequent extrusion cycles, J. Appl. Polym. Sci. 131 (6) (2014) (n/a-n/a).
[3] L.T. Lim, R. Auras, M. Rubino, Processing technologies for poly(lactic acid), Prog. Polym. Sci. 33 (8) (2008) 820.
[4] I. Pillin, N. Montrelay, A. Bourmaud, Y. Grohens, Effect of thermo-mechanical cycles on the physico-chemical properties of poly(lactic acid), Polym. Degrad. Stab. 93 (2) (2008) 321.
[5] C. Bastioli, R.T. Limited, Handbook of Biodegradable Polymers, Rapra Technology, 2005.
[6] [a] W. Klöpffer, B. Grahl, Life Cycle Assessment (LCA), Wiley, 2014; [b] J.D. Badía, E. Strömberg, A. Ribes-Greus, S. Karlsson, Assessing the MALDITOF MS sample preparation procedure to analyze the influence of thermooxidative ageing and thermo-mechanical degradation on poly (lactide), Eur. Polym. J. 47 (7) (2011) 1416.
[7] [a] Y. Fan, H. Nishida, Y. Shirai, Y. Tokiwa, T. Endo, Thermal degradation behaviour of poly(lactic acid) stereocomplex, Polym. Degrad. Stab. 86 (2) (2004) 197; [b] V. Taubner, R. Shishoo, Influence of processing parameters on the degradation of poly (L-lactide) during extrusion, J. Appl. Polym. Sci. 79 (12) (2001) 2128.
[8] [a] M. Gupta, V. Deshmukh, Thermal oxidative-degradation of poly-lactic acid. 1. Activation-energy of thermal-degradation in air, Colloid Polym. Sci. 260 (3) (1982) 308-311;
[b] S.H. Hyon, K. Jamshidi, Y. Ikada, Effects of residual monomer on the degradation of DL-lactide polymer, Polym. Int. 46 (3) (1998) 196; [c] K. Madhavan Nampoothiri, N.R. Nair, R.P. John, An overview of the recent developments in polylactide (PLA) research, Bioresour. Technol. 101 (22) (2010) 8493.
[9] F. Carrasco, P. Pagès, J. Gámez-Pérez, O.O. Santana, M.L. Maspoch, Processing of poly(lactic acid): characterization of chemical structure, thermal stability and mechanical properties, Polym. Degrad. Stab. 95 (2) (2010) 116.
[10] R. Al-Itry, K. Lamnawar, A. Maazouz, Improvement of thermal stability, rheological and mechanical properties of PLA, PBAT and their blends by reactive extrusion with functionalized epoxy, Polym. Degrad. Stab. 97 (10) (2012) 1898.
[11] R. Pantani, F. De Santis, A. Sorrentino, F. De Maio, G. Titomanlio, Crystallization kinetics of virgin and processed poly (lactic acid), Polym. Degrad. Stab. 95 (7) (2010) 1148.
[12] J.D. Badia, E. Strömberg, S. Karlsson, A. Ribes-Greus, Material valorisation of amorphous polylactide. Influence of thermo-mechanical degradation on the morphology, segmental dynamics, thermal and mechanical performance, Polym. Degrad. Stab. 97 (4) (2012) 670.
[13] [a] F. Carrasco, J. Gámez-Pérez, O.O. Santana, M.L. Maspoch, Processing of poly(lactic acid)/organomontmorillonite nanocomposites: microstructure, thermal stability and kinetics of the thermal decomposition, Chem. Eng. J. 178 (0) (2011) 451; [b] P. Cerruti, C. Carfagna, Thermal-oxidative degradation of polyamide 6,6 containing

metal salts, Polym. Degrad. Stab. 95 (12) (2010) 2405.
[14] A. Csikós, G. Faludi, A. Domján, K. Renner, J. Móczó, B. Pukánszky, Modification of interfacial adhesion with a functionalized polymer in PLA/wood composites, Eur. Polym. J. 68 (2015) 592.
[15] S. Sabnis, L. Block, Improved infrared spectroscopic method for the analysis of degree of N-deacetylation of chitosan, Polym. Bull. 39 (1) (1997) 67.
[16] Q. Zhou, M. Xanthos, Nanosize and microsize clay effects on the kinetics of the thermal degradation of polylactides, Polym. Degrad. Stab. 94 (3) (2009) 327.
[17] K. Fukushima, D. Tabuani, M. Dottori, I. Armentano, J. Kenny, G. Camino, Effect of temperature and nanoparticle type on hydrolytic degradation of poly(lactic acid) nanocomposites, Polym. Degrad. Stab. 96 (12) (2011) 2120.
[18] X. Liu, Y. Zou, W. Li, G. Cao, W. Chen, Kinetics of thermo-oxidative and thermal degradation of poly(d,l-lactide) (PDLLA) at processing temperature, Polym. Degrad. Stab. 91 (12) (2006) 3259.
[19] Y.X. Weng, L. Wang, M. Zhang, X.L. Wang, Y.Z. Wang, Biodegradation behavior of P(3HB,4HB) /PLA blends in real soil environments, Polym. Test. 32 (1) (2013) 60.
[20] [a] L. Zaidi, M. Kaci, S. Bruzaud, A. Bourmaud, Y. Grohens, Effect of natural weather on the structure and properties of polylactide/Cloisite 30B nanocomposites, Polym. Degrad. Stab. 95 (9) (2010) 1751;
[b] A. Araújo, G. Botelho, M. Oliveira, A.V. Machado, Influence of clay organic modifier on the thermal-stability of PLA based nanocomposites, Appl. Clay Sci. 88-89 (0) (2014) 144.
[21] I.C. McNeill, H.A. Leiper, Degradation studies of some polyesters and polycarbonates-2. Polylactide: degradation under isothermal conditions, thermal degradation mechanism and photolysis of the polymer, Polym. Degrad. Stab. 11 (4) (1985) 309.
[22] M. Gardette, S. Thérias, J.L. Gardette, M. Murariu, P. Dubois, Photooxidation of polylactide/calcium sulphate composites, Polym. Degrad. Stab. 96 (4) (2011) 616.